Joint Reinforcement as Primary Shear Reinforcement for Concrete Masonry Shear Walls

Greg Baenziger[1] and Max L. Porter[2]

INTRODUCTION

Partially grouted masonry shear walls are common in North America. Construction of partially grouted concrete masonry shear walls can benefit greatly by placement of joint reinforcement in bed joints of each or every other course instead of deformed reinforcement in bond beams, because placement and grouting of bond beams slow construction. Joint reinforcement is already used to help control cracking and provide prescriptive horizontal reinforcement. With sufficient area and ductility of wire, joint reinforcement can also provide the tension capacity to span across cracks in shear walls and to act as primary shear reinforcement for in-plane shear forces.

The research reported herein provides:

1. direct comparisons of walls constructed using joint reinforcement as shear reinforcement and walls constructed using conventional deformed reinforcement in bond beams;
2. demonstration of shear wall behavior with joint reinforcement as primary shear reinforcement;
3. demonstration that wire reinforcement can be provided with sufficient area and ductility to avoid fracture;
4. further demonstration of the validity of the Schultz (Schultz 1996) strength and energy criteria; and
5. further expansion of the database of tests of full-size shear walls, including partially grouted walls.

BACKGROUND

In early shear wall tests of fully grouted masonry walls, there was a presumption that the higher strength of cold drawn wire used in joint reinforcement would result in reduced cross-sectional areas of steel required. Testing was carried out with small areas of joint reinforcement, which resulted in fractured wires. As a result, there was apprehension in using joint reinforcement to resist shear loads. Early shear wall tests included tests by Shing (1991 and 1992) and Sveinsson (1985), carried out with fully grouted walls.

Sveinsson (1985) conducted tests that included wire truss joint reinforcement in every bed joint of small piers as horizontal shear reinforcement. Sveinsson stated that the joint reinforcement did not provide the strength that the two #5 (M#16) bars provided in the comparison wall; however, the areas of reinforcement were not comparable. The longitudinal wires of six effective joint reinforcement wire trusses had a total cross-sectional area of 0.33 in.^{2} (213 mm^2) compared to the two #5 (M#16) bars, which had a total cross-sectional area of 0.62 in.^{2} (400 mm^2). Sveinsson did suggest that joint reinforcement enhanced the ductility of the piers, which is an important property of shear walls for resisting collapse.

Shing (1991 and 1992) documented the study of two cantilever wall panels, Wall D1, which used heat-treated joint reinforcement and, Wall D2, which used cold-drawn joint reinforcement. The walls were tested under the TCCMAR program in the same manner as Sveinsson's study and were compared to Wall 14 of the earlier work by Shing, which did not include joint reinforcement. All walls were 6-foot (1.83-m) square fully grouted concrete masonry walls $5^5/_8$ inches (143 mm) thick. All walls were subjected to a 270 psi (1.86 MPa) compressive surcharge. Walls D1 and D2 were constructed with ladder style joint reinforcement in each bed joint, 0.15-inch (3.76-mm) diameter wire (9-gage), and a total horizontal wire area of 0.275 in.^{2} (177 mm^2). Wall 14 was constructed with #3 (M#13) bars at 16-inch (406-mm) spacing with a total bar area of 0.55 in.^{2} (355 mm^2), double the reinforcement area of Walls D1 and D2.

All three walls exhibited brittle shear failures. Wall capacities and shear load at failure were significantly greater than horizontal reinforcement capacities. The wall with heat treated wire ruptured at 104 kips (464 KN), where total wire capacity was 23 kips (102 KN) yield and 25 kips (111 KN) ultimate. The wall with cold-drawn wire ruptured at 102 kips (452 KN), where total wire capacity was 26 kips (116 KN) yield and 27 kips (120 KN) ultimate. The wall with deformed reinforcement ruptured at 94 kips (418 KN), notably less than the walls with joint reinforcement. The bar capacity was 31 kips (138 KN) yield and 45 kips (200 KN) ultimate. Shing reported that the brittle behavior of all three walls studied was due to the small quantity of horizontal reinforcement.

1. P.E., Former Graduate Research Assistant, Dept. of Civil, Construction, and Environmental Engineering, Iowa State University, Ames, IA, gbaenzig@gmail.com
2. Ph.D., P.E., TMS Fellow Member, Professor Emeritus, Dept. of Civil, Construction, and Environmental Engineering, Iowa State University, Ames, Iowa, mporter@iastate.edu

Additional tests were conducted in cooperation with The National Institute of Standards and Technology (NIST) by Schultz (1994, 1998 and 2001) with partially grouted walls. Test walls used 0.148-inch (3.76 mm) 9-gage or 0.207-inch (5.26 mm) 5-gage wire. Three aspect ratios were tested: 56 inches (1.42 m) high by 112, 80, and 56 inches (2.84, 2.03, and 1.42 m) long. Schultz (2001) reported that partially grouted shear walls using sufficient horizontal joint reinforcement performed well. The walls generated large lateral drifts prior to deteriorating and thus were able to dissipate energy through inelastic deformations. Schultz concluded that joint reinforcement met the tensile requirements for shear reinforcement and helped to make partially grouted walls a viable, stable lateral-load resisting system for seismic design, with high initial stiffness and ample energy dissipation. The failure of the walls included fracture of wires, but the failure was reported to be:

> "…gradual, as progressive damage was being accumulated by these moderately resilient walls which exhibited a respectable amount of toughness." (Schultz 2001)

> "The lateral load resisting mechanism observed in the tests represents a considerable improvement over that observed for the partially-grouted shear walls with bond beams in the previous phase of the experimental program (Schultz 1994)." (Schultz 2001)

NIST tests combined with research reported here from Iowa State University (Braun 1997) and (Baenziger 2010 and 2011) have shown that sufficient areas of joint reinforcement can satisfy strength and energy criteria by Schultz (1996), and can resist shear in masonry walls without fracture of reinforcement.

EXPERIMENTAL PROGRAM

The research included construction and testing of ten full-size concrete masonry cantilever shear walls, as indicated in Table 1. The tests by Baenziger (2010 and 2011) included both partially grouted and fully grouted walls. The walls were 8'-8" (2.64 m) high and either 9'-4" (2.85 m) long, as shown in Figure 1, or 14'-0" (4.27 m) long, providing two aspect ratios (Height/Length) 0.93 and 0.62. No surcharge loading was applied to the walls. The top of the wall was allowed to rotate in-plane as a cantilever, indicated in Figure 2. Test Groups A and D were designed as shear-dominant walls similar to previous tests of shear reinforcement. Test Groups B and C were designed as flexural walls approximating code based designs consistent with capacity design, providing flexural yielding before failure, and developing plastic hinges.

Joint reinforcement conforming to ASTM A951 was either single ladder style or double seismic style placed in every bed joint. Wires were hot dip galvanized. The longitudinal wires were 3/16-inch (4.8-mm) diameter cold-drawn wire. Crosswires were 9-gage wires butt welded to the longitudinal wires at 16-inch (406-mm) spacing. Deformed reinforcement consisted of two #4 (M#13) Grade 60 bars located in bond beams at 48-inch (1.22-m) spacing. Horizontal reinforcement, illustrated in Figure 3 with properties provided in Table 2, had 90° or 180° hooks at the ends bent around but not in contact with the vertical jamb reinforcement. Vertical reinforcement was #4 (M#13) or #6 (M#19) Grade 60 threaded splice bars located in grouted cells at a maximum spacing of 48 inches (1.22 m) with 90° bend and threaded splice embedded in the concrete base.

Masonry was: ASTM C90 8-inch (203-mm) concrete masonry units with 8-inch (203-mm) courses and cell spacing; ASTM C270 Spec Mix Portland Cement-Lime-Sand Mortar; and ASTM C476 Spec Mix Corefill Grout.

Table 1. Test Matrix for Shear Wall Program

Group	A	B	C	D
Dominance	Shear	Flexure		Shear
Aspect Ratio (H/L)	0.93			0.62
Grout	Part		Full	Part
Vertical / Horizontal	2#6 (M#19)	2#4 (M#13)	2#4 (M#13)	2#6 (M#19)
2#4(M#13) DR Bond Beam	SW1	SW7	SW9	SW3
2x3/16"(4.8mm) JR Wire	SW2	SW5		SW4
4x3/16"(4.8mm) JR Wire	SW6		SW10	SW8

DR – Deformed Reinforcement SW# – Shear Wall ID
JR – Joint Reinforcement

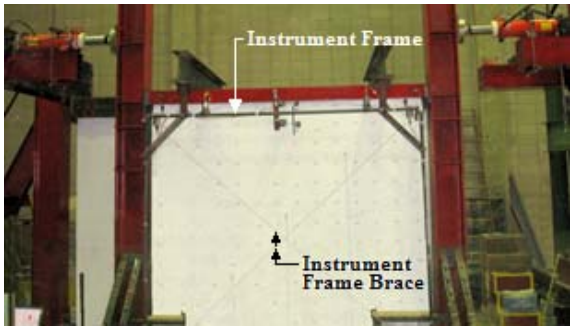

Figure 1 – Typical Test Wall, Test Frame, Load Actuators, and Instrumentation

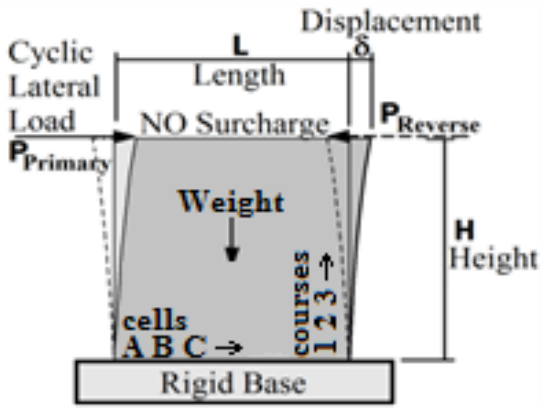

Figure 2 – Shear Wall Configuration

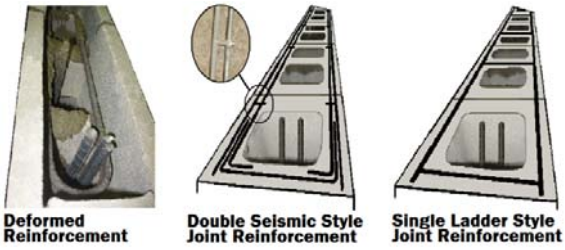

Figure 3 – Horizontal Shear Reinforcement Images

Table 2. Reinforcement Properties

Reinforcement		Yield		Maximum	
		Stress	Strain	Stress	Strain[1]
		psi (MPa)		psi (MPa)	
Horizontal	Grade 60 #4 (M#13) DR Bar	64,480 (444.6)	0.00242	103,330 (712.4)	0.0948[2]
	3/16"(4.8mm) JR Wire	87,950 (606.4)	0.00288	91,060[2] (627.8)	0.0609[3]
Vertical	Grade 60 #6 (M#19) DR Bar	63,190 (435.7)	0.00238	101,400 (699.1)	0.0915
	Grade 60 #4 (M#13) DR Bar	66,980 (461.8)	0.00298	104,250 (718.8)	0.0888

[1]Maximum strains were at maximum stress
[2]Ultimate strain averaged 0.1138
[3]Ultimate strain values were equal to strains at maximum stress

Nominal design strength was 1,500 psi (10.3 MPa). Actual compressive strength, for ASTM C1314 moist-cured prisms, $f'_{m\text{-}prism}$, averaged between 2,500 psi (17.2 MPa) and 3,530 psi (24.3 MPa). There was no significant difference between ungrouted and grouted prism strengths once the net area was considered. Grout strength varied between 2,650 psi (18.3 MPa) and 5,640 psi (38.9 MPa). The mortar was ASTM C270 Type S by proportion. ASTM C109 mortar strength varied between 1,120 psi (7.7 MPa) and 1,760 psi (12.1 MPa). Wet cured prism strengths were within 3.5% of the average for a group, with the exceptions of Shear Wall 7 in Group B and Shear Wall 8 in Group D. The prism strength of Shear Wall 7 was 10.7% greater than the average prism strength and 23.9% greater than that of Shear Wall 5. The Shear Wall 8 prism strength was 12.3% greater than the average strength of the group.

Instrumentation consisted of load cells, strain gages, and string potentiometers. Potentiometers were attached to the concrete base and to the braced instrument frame, which was supported by the concrete base. The instrument support frame is visible at the periphery of the test wall in Figure 1, and the hydraulic actuators and load cells are visible in the upper corners. The mechanism for load transfer is illustrated in Figure 4. Horizontal loads were applied slowly at the top of the cantilever shear walls using displacement control and following the procedure recommended by the U.S. Coordinated Program for Masonry Building Research and the Technical Coordinating Committee for Masonry Research (TCCMAR) (Porter 1987). The load sequence, illustrated in Figure 5, consisted of sets of three cycles at increasing displacements until a major event, such as significant cracking, occurred followed by sets of degradation cycles, three stabilization cycles, and an increased displacement cycle until the wall failed.

In the first two test walls, vertical reinforcement extended into the top bond beam past the horizontal bars but did not have a bend or hook. In subsequent walls, ¾-inch (19-mm) threaded rods were embedded 24 inches (610 mm) into the top jamb cells and anchored to the cap beam and #4 (M#13) bent bars were lapped with each vertical bar and anchored above the top horizontal bars. Also, a second jamb cell was reinforced and grouted. The improved configuration in the last eight walls was to prevent internal vertical reinforcement anchorage failures at the top of the wall and delamination of the jamb. Common to all walls were one-inch (25.4-mm) diameter bolt anchors fastened to the cap beam in each top cell.

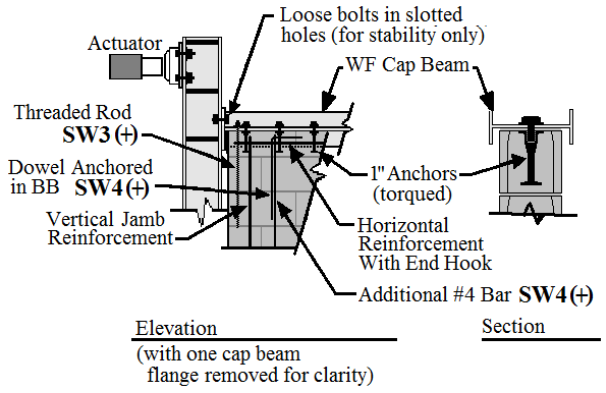

Figure 4 – Cap Beam and Reinforcement Anchorage Illustrations

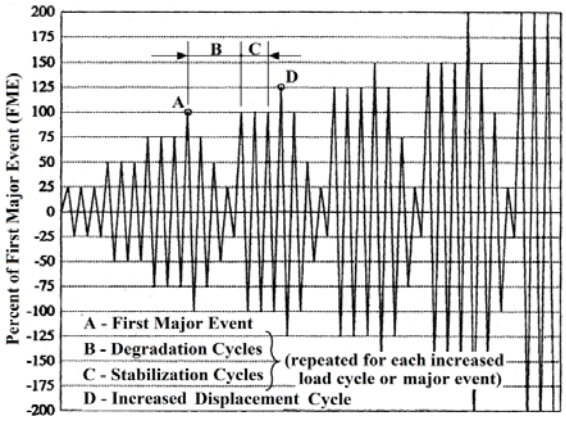

Figure 5 – TCCMAR Cyclic Loading Pattern

RESULTS AND OBSERVATIONS

Maximum lateral load, displacement at peak load, wall configuration, and material test data are provided in Table 3. Groups A and D were designed to demonstrate "shear critical behavior" and the capacity of the horizontal shear reinforcement by including greater cross-sectional areas of vertical reinforcement referred to as "full vertical reinforcement." Groups B and C were designed as "capacity design" walls with reduced vertical flexural reinforcement cross-sectional areas, configured to limit the overstrength of the walls. In high seismic demand zones, walls in Wall Group A would be inappropriate designs due to high overstrength and would result in undesirable brittle shear wall failures.

WALL GROUP A – Performance of Partially Grouted, Shear-Critical Walls with High Aspect Ratio

Shear Wall 1, H/L=0.93, with 2 #4 (M#13) bars in a mid-height bond beam, had horizontal flexural crack origin moving up the jambs followed by diagonal cracking at the upper corner beneath the top bond beam and moving further along the top of the wall, typical for the test walls. The horizontal bars, in the mid-height bond beam, did not yield and restrained crack sizes along the bond beam. There was greater deformation and cracking above mid-height. At approximately 60% of capacity, a large diagonal crack formed in the primary loading direction, Figure 6(a). Due to the release of the top vertical jamb bar anchorage, strength was limited in the primary direction. Reverse loading continued to full capacity, Figure 6(b). The top anchorage failure resulted in a loading plateau between 0.1 and 0.65 inches (3 and 17 mm) displacement and reduced energy dissipation, with the mid-wall vertical reinforcement acting as a spring. The lack of plastic deformation in the primary direction was one reason for greater capacity in the reverse direction, where mostly monotonic loading occurred. Tests were halted when sliding resulted in the loss of stability of the top courses, limiting overall displacement to about 2 inches (51 mm).

Shear Wall 2, with 3/16-inch (4.8-mm) single ladder style joint reinforcement in every bed joint, demonstrated more uniform cracking, both in size and distribution, Figure 6(c), and better engagement of the shear reinforcement than did Shear Wall 1. The joint reinforcement wire strain reached 0.003483, which is 21% greater than the yield strain.

Shear Wall 6, with 3/16-inch (4.8-mm) double seismic style joint reinforcement in every bed joint, behaved more robustly than Shear Walls 1 and 2. Shear Wall 6 demonstrated a greater level of shear capacity and ductility. Shear Wall 6 had greater areas of well-distributed reinforcement to restrict the crack size and distribute deformations uniformly across the wall. The load-displacement diagram for Shear Wall 6 is provided in Figure 7.

Table 3. Experimental Average Maximum (Peak) Shear Capacities[1]

Group	Wall	Reinforcement	Avg. Peak Shear[1]		Avg. Displacement @Peak[1]		Gross $\rho_{horz.}$ %	Jamb Bars[3]	Gross ρ_{Vert}[2] %	Aspect Ratio H/L	Grout	Avg. Net Area		Avg. Wet Prism Strength $f'_{m\ prism}$	
			kips	KN	in.	mm						in.^{2}	cm^2	ksi	MPa
A	1	DR – 2x #4 (M#13)	46.8	208	0.482	12.2	0.109	2	0.24	0.93	Partial	520.5	3358	2.72	18.8
	2	JR – 2x $^3/_{16}$"(4.8 mm)	45.2	201	0.352	8.9	0.091		0.25			520.5	3358	2.72	18.8
	6	JR – 4x $^3/_{16}$"(4.8 mm)	73.2	326	0.424	10.8	0.181		0.29			587.2	3788	2.85	19.6
B	7	DR – 2x #4 (M#13)	56.0	249	0.310	7.9	0.109	1	0.19			587.2	3788	3.53	24.3
	5	JR – 2x $^3/_{16}$"(4.8 mm)	59.8	266	0.470	11.9	0.091		0.19			587.2	3788	2.85	19.6
C	9	DR – 2x #4 (M#13)	95.6	425	0.956	24.3	0.109		0.29		Full	854.0	5510	3.11	21.4
	10	JR – 4x $^3/_{16}$"(4.8 mm)	95.4	424	0.642	16.3	0.181		0.28			854.0	5510	2.90	20.0
D	3	DR – 2x #4 (M#13)	78.3	348	0.333	8.5	0.109	2	0.20	0.62	Partial	780.6	5036	2.72	18.8
	4	JR – 2x $^3/_{16}$"(4.8 mm)	96.9	431	0.492	12.5	0.091		0.23			847.5	5468	2.86	19.7
	8	JR – 4x $^3/_{16}$"(4.8 mm)	91.2	406	0.334	8.5	0.181		0.23			847.5	5468	3.34	23.0

[1]Averaged between primary and reverse load directions

[2]Number of vertical #6 (M#19) bars (or equivalent) located in the jamb. One #4 (M#13) was located in certain cells other than the jamb. Reinforcement was located in: cells A-G-H-N for Shear Wall 1 (SW1) and SW2; cells A-B-G-H-M-N for SW5, SW6, and SW7; cells A-B-D-E-G-H-J-K-M-N for SW9 and SW10; cells A-G-H-N-O-U for SW3; and cells A-B-G-H-N-O-T-U for SW4 and SW8.

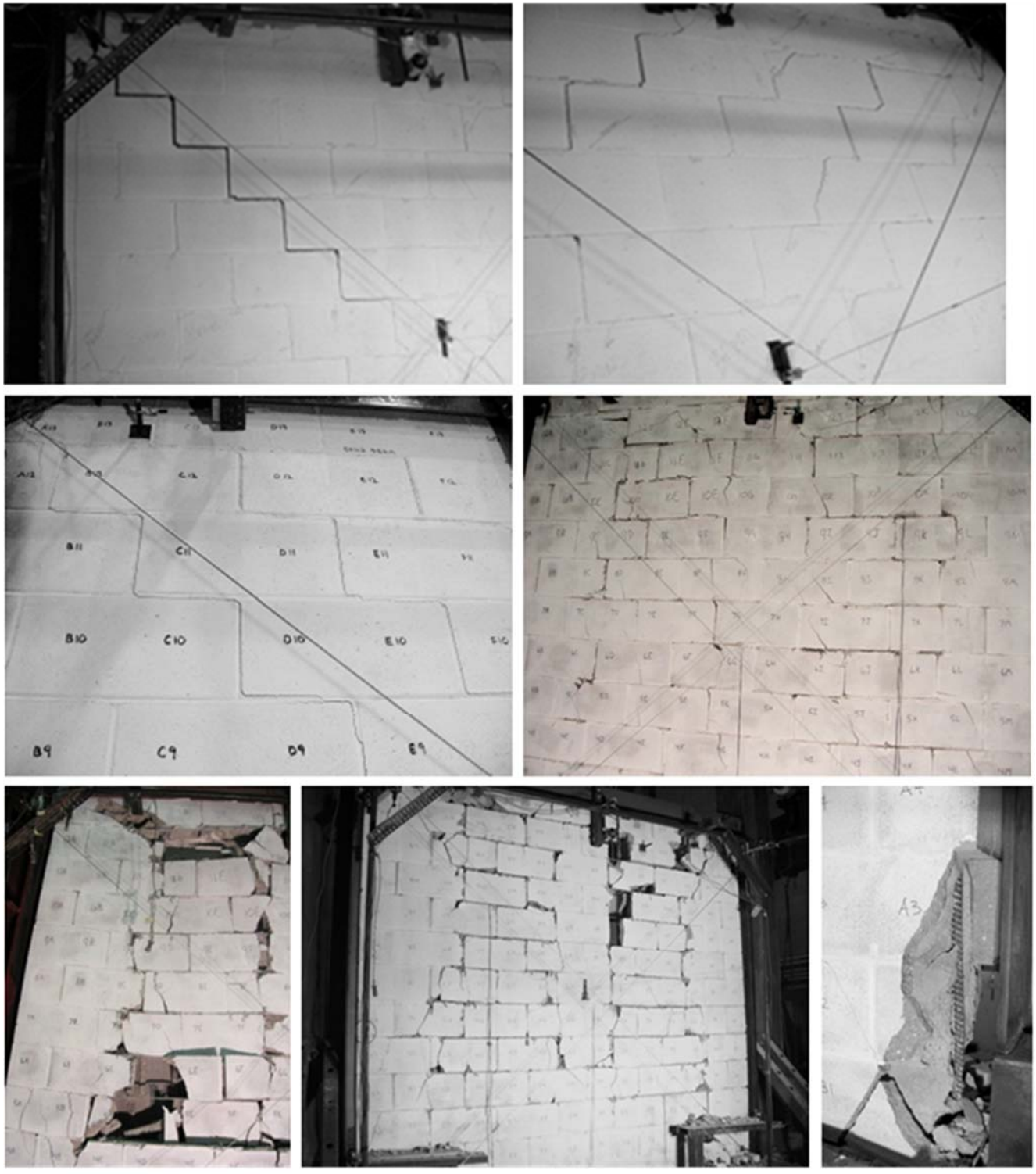

Figure 6 – (a) SW1 Primary Diagonal Crack (upper left); (b) Reverse Load Cracks (upper right); (c) SW2 Stair Step Cracking (middle left); (d) SW6 Ungrouted Panel Cracking at 68.6 kips (305 KN) Load and 0.6 in. (15.2 mm) Displacement (middle right); (e) SW6 at 5 in. (127 mm) Displacement (bottom left); (f) SW5 Ungrouted Panel Damage at 5 in. (127 mm) Displacement (bottom middle); and (g) SW9 Damage Due to Sliding at 88 kips (391 KN) and 1 in. (25.4 mm) Displacement (bottom right)

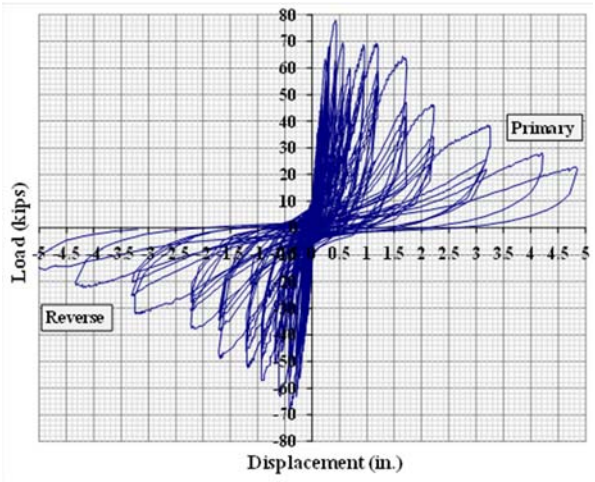

Figure 7 – Shear Wall 6 Load-Displacement

The improved anchorage at the top of the wall and the second jamb cell increased initial stiffness and added to the greater strength of the wall after significant damage to the ungrouted panels. The moment resistance of the reinforced and grouted cells around the ungrouted panels helped to prolong the wall strength and increase drift capacity. Two stages of wall damage are shown in Figures 6(d) and 6(e), maximum shear capacity and maximum wall displacement, respectively. Shear Wall 6 was not directly comparable to the other walls of the group, but the test demonstrated the possible increase in capacity and displacement due to greater areas of horizontal joint reinforcement distributed at a small spacing with improved wall details to include top hooks.

WALL GROUP B – Performance of Partially Grouted, Flexure-Critical Walls with High Aspect Ratio

Shear Wall 5, H/L=0.93, with 3/16-inch (4.8-mm) single ladder style joint reinforcement in each bed joint, was similar to Shear Wall 6. Increased flexural deformations were apparent and included plastic deformation of the vertical jamb reinforcement up to and beyond the onset of strain-hardening. The test proceeded to approximately 5 inches (127 mm) displacement demonstrating pronounced masonry cell frame behavior of the stronger reinforced and grouted cells around the ungrouted panels. The joint reinforcement remained intact and provided a stabilizing effect for the lower strength masonry wall. The broader load-displacement loops in Figure 8(a) indicate a more robust energy dissipation capacity and ductility associated with shear walls that have reserve capacity after significant displacement. Cracking in Shear Wall 5 is illustrated in Figure 6(f).

Shear Wall 7, with 2 #4 (M#13) bars in a mid-height bond beam, was similar to other bond beam walls, with a significant diagonal crack that opened after 0.6 inches (15.2 mm) displacement in the reverse direction. Sliding and delamination occurred after displacements exceeded one inch (25 mm), in Figure 9(a). The mid-height bars restrained cracking, but the bond beam acted as a strut contributing to delamination at each end. The greater prism strength of Shear Wall 7 over Shear Wall 5 is not reflected in the overall wall peak shear capacity (93.6% of that of Shear Wall 5). Increased loads, resulted in sliding and interaction with the test frame, visible in the bottom left of the load-displacement graph beyond -1.5 inches (38.1 mm) displacement, Figure 8(b).

WALL GROUP C – Performance of Fully Grouted, Flexure-Critical Walls with High Aspect Ratio

Shear Wall 9, H/L=0.93, a fully grouted wall with 2 #4 (M#13) bars in a mid-height bond beam, showed improved crack distribution over partially grouted walls and a greater number of smaller cracks. Fracture of the #6 (M#19) vertical bar above the threads in the threaded splice at the base occurred during loading in the reverse direction. Shear Wall 9 could not be tested in the reverse direction beyond one inch (25 mm) displacement due to sliding damage, shown in Figure 6(g), and instability. The wall remained stable longer in the primary loading direction with the largest diagonal crack shown in Figures 9(b) and 9(c). The gap between wall and base at the bottom right of Figure 9(c) was due to plastic deformation of the vertical reinforcement. The wall strength dropped significantly and became unstable beyond three inches displacement in the primary direction due to loss of dowel resistance.

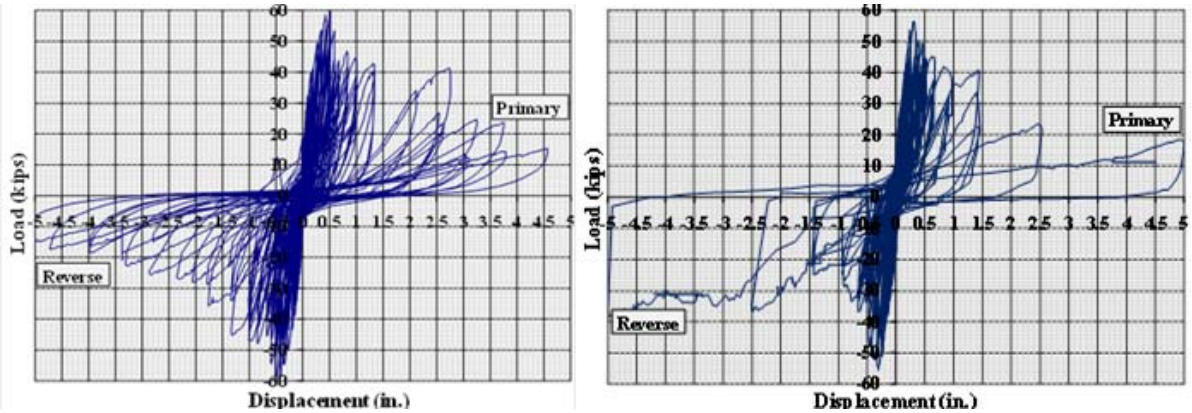

Figure 8 – Load-Displacement Plots: (a) Shear Wall 5 (left) and (b) Shear Wall 7 (right)

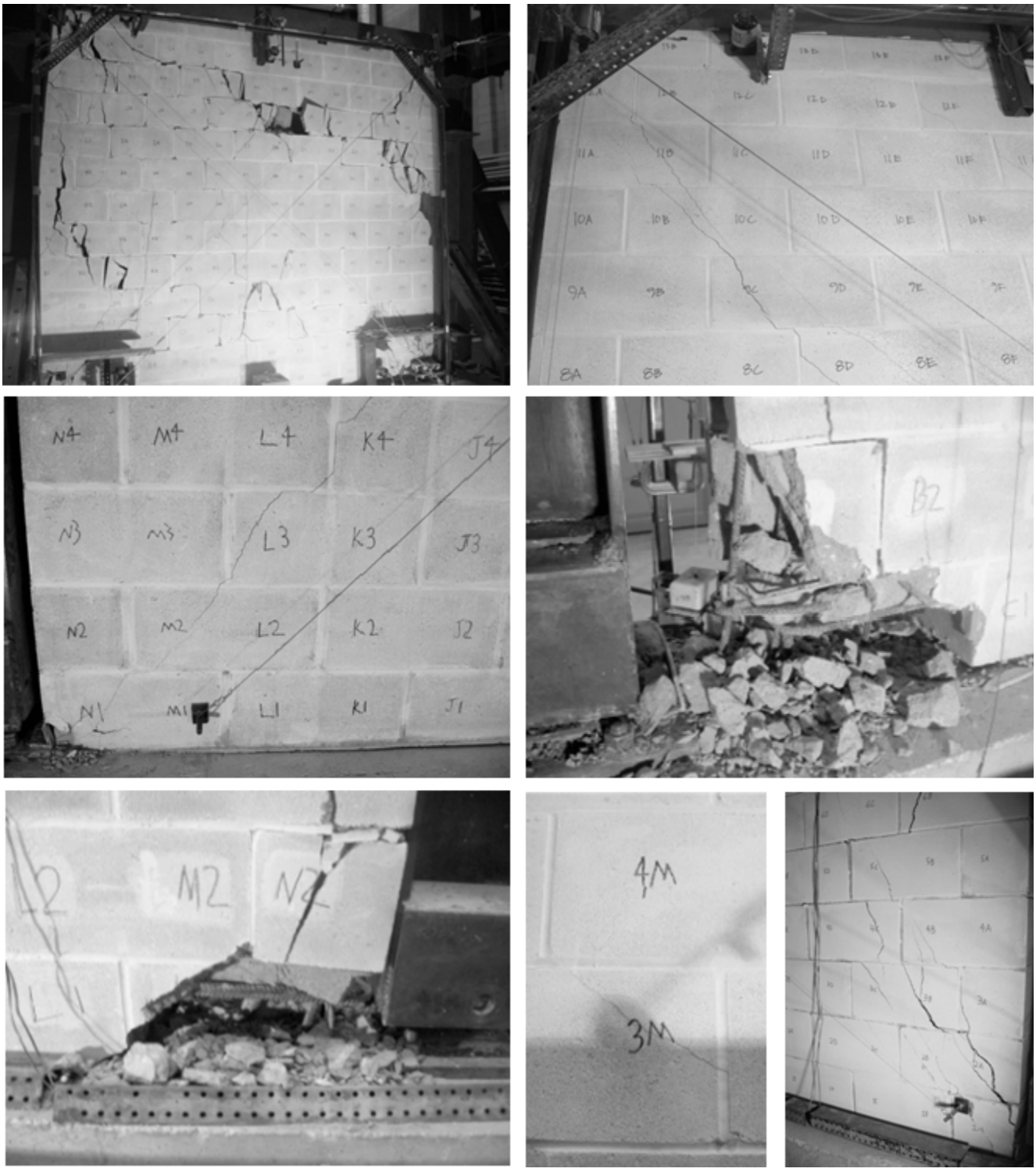

Figure 9 – (a) SW7 at 5 in. (127 mm) Displacement with Mid-Height Bond Beam (top left); (b) SW9 Diagonal Cracks (top right) and (c) at 103 kips (458 KN) Load and 1.5 in. (38 mm) Displacement, Seen from Opposite Sides of the Wall (middle left); (d) SW10 Toe Crushing (Double Joint Reinforcement, middle right); (e) SW10 (Double Joint Reinforcement) Compression at 4 in. (102 mm) Displacement (bottom left); 17 (f) SW10 (Double Joint Reinforcement) Largest Crack at 96 kips (427 KN) load and 0.85 in. (22 mm) Displacement (bottom middle); and (g) SW4 Beyond Peak Load with Diagonal Cracks Extending to the Base (bottom right)

Shear Wall 10, with 3/16-inch (4.8-mm) double seismic style joint reinforcement in every bed joint, was similar to Shear Wall 9, except without the fracture of the vertical bar. Significant deformation of the vertical bars occurred at the base of the wall due to the dowel resistance contribution near failure. The average horizontal reinforcement peak strain was 62% of yield. Displacements and ductility were due to vertical bar plastic elongation beyond strain hardening and sliding. The wall continued to resist nearly half the peak shear capacity after sliding but was not stable beyond 4 inches displacement in the reverse direction.

Both fully grouted shear walls provided significant shear resistance throughout the tests, and the masonry remained intact except at the base. Damage to the vertical bar dowel anchorage at the base and the resulting instability was the primary reason for terminating both tests. Restraint of the vertical bars by the bottom bond beam reinforcement continued through 2 inches of wall displacement. At greater displacement, grout failure around the bars allowed increasing deformation, Figures 9(d) and 9(e). Both walls lost shear resistance due to failure to recompress deformed vertical steel at the base upon load reversal. In both shear walls, displacements beyond one inch were increasingly due to sliding.

WALL GROUP D – Performance of Partially Grouted, Shear-Critical Walls with Low Aspect Ratio

Shear Wall 3, H/L=0.62, with 2 #4 (M#13) bars in a mid-height bond beam, behaved similarly to Shear Wall 1, with cracking in fewer larger cracks, shown in Figure 10(a). Eventually, the delamination of the jambs, visible to the right in the figure, degraded wall behavior and resulted in a failure plane combining diagonal cracking and sliding adjacent to the bond beam.

Shear Wall 4, with 3/16-inch (4.8-mm) single ladder style joint reinforcement in every bed joint, was similar to Shear Wall 3. The added reinforced and grouted jamb cells increased the strength and displacement capacity and delayed jamb delamination and sliding. An extension of the diagonal cracking at the base can be seen in Figure 9(g). Six cross wires fractured at the wall ends due to vertical movement, and one tension failure of a side rail mid-height at one jamb were observed, all due to jamb delamination. Shear wall 4 experienced the greatest joint reinforcement strains of all of the walls. On the wall diagonal at the lower quarter point, strains reached approximately one-third of the ultimate strain capacity of the wire, which was eight times the yield strain.

Shear Wall 8, with 3/16-inch (4.8-mm) double seismic style joint reinforcement in every bed joint, was similar to the other walls in the group, except with better crack distribution and smaller cracks, as illustrated in Figure 10(b). The shear capacity was similar to Shear Wall 4, but the strains were significantly smaller. The Shear Wall 8 peak shear capacity was 16.5% greater than that of Shear Wall 3, but only 94% of that of Shear Wall 4. Cracking was nearly vertical occurring in face shells as well as mortar joints and located primarily in the ungrouted panels adjacent to grouted cells. The visible cracking of the bed joints in the top courses preceded the onset of sliding there.

In Group D walls, the vertical reinforcement did not experience the extent of plastic deformations experienced by the walls with reduced vertical reinforcement in Groups B and C, and thus do not have the loss of shear resistance in failing to recompress the vertical steel upon load reversal. The degradation in shear capacity was a result of the degradation of masonry, which occurred to a greater degree in the ungrouted regions of the walls. The walls with joint reinforcement had greater shear capacity and ductility, in part because more uniform distribution of horizontal reinforcement maintained the integrity of the masonry and delayed damage which results in the formation of failure planes. Shear Wall 8 did not provide greater capacity than Shear Wall 4 because the additional area of wire was not required for strength. Shear Wall 8 experienced smaller reinforcement strains and as a result demonstrated greater ductility than Shear Wall 4.

Shear Wall Strengths and Displacements

Peak shear capacity and displacement are used to evaluate shear wall performance. Table 4 provides the shear wall capacities at various displacements and drift levels. Masonry shear wall capacities reported by past research have been shown to be significantly below the design capacities predicted by code criteria. The disparity is primarily due to the use of wet-prism strengths to correlate strength of the test walls, which were used in these tests. Based on data from Schultz and Hutchinson (2001) which tested both moist-cured and air-cured prisms, the air-cured prisms had 77.6% of the capacity of moist-cured prisms, a reduction of 22.4% in actual experimental data, resulting in a ratio of 1.29 as a correction factor. Harris (2010) also reported 62.9% of capacity based on similar data. Shear wall capacities based on air-cured prism tests, cured next to the walls would have been nearer their predicted capacities.

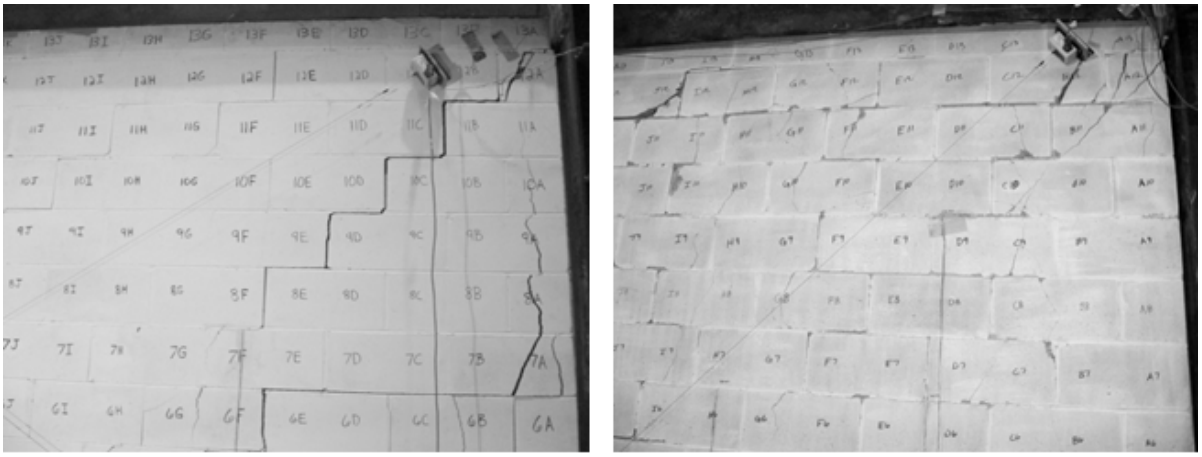

Figure 10 – (a) Shear Wall 3 Restrained Cracks at Mid-Height Bond Beam (course 7) beyond Peak Load (left) and (b) Shear Wall 8 Beyond Peak Load (right)

Modes of Failure and Sliding

The first two tests demonstrated undesirable failure modes including a vertical bar top anchorage failure, delamination of the jamb, and sliding after peak loading. Additional vertical anchorage was added to the top of Shear Wall 3 to delay undesirable failure modes. For all subsequent walls, additional top anchorage was installed and a second jamb cell was reinforced and grouted.

The shear wall tests were carried out up to 5 inches (127 mm) displacement to determine the complete pattern of failure. The walls with joint reinforcement and bond beams resulted in no failures of the longitudinal wires attributed to diagonal shear cracking. The primary mode of failure in the partially grouted walls was masonry damage, including both horizontal and diagonal cracking.

Significant load resistance was observed for large levels of drift, especially in the partially grouted, Shear Walls 5 and 7, with reduced areas of jamb flexural reinforcement to limit overstrength per FEMA P695 (ATC (2009)). There was a rebound or plateau in strength after shear resistance decreased as flexure of the reinforced and grouted cells, dominated the resistance to displacement. The walls experienced significant plastic deformation of the vertical bars. Greater drift capacity than other shear dominated walls was also observed in the Shear Wall 6, with double joint reinforcement. The uniform distribution of shear reinforcement and the greater area of wire combined with flexure of the reinforced and grouted cells improved drift capacity.

The cumulative cracking resulted in planes of failure due to large flexural deformations and insufficient compression force in the reverse cycle to recompress the vertical steel upon load reversal and to close flexural cracks each cycle. The lack of full contact between masonry crack surfaces resulted in low shear friction and decreased shear resistance. Eventually, sliding occurred along the damaged failure surfaces. From Table 5, the displacement ductility can be seen to vary significantly between inclusion and exclusion of sliding.

Table 4. Average Shear Capacity at Drift[1] and Displacements at Peak Shear Capacity With and Without Sliding

Group	Wall	Horizontal Reinforcement	ρ	Shear @ Drift[2]						Displacements at Peak					
				0.007		0.01		0.02		W/Sliding		Sliding		W/O Sliding	
				kips	KN	kips	KN	kips	KN	in.	mm	in.	mm	in.	mm
A	1	DR Bars	0.11	28	125	18	80	*[4]	*[4]	0.327[5]	8.31	0.015[5]	0.38	0.312[5]	7.92
	2	Single JR	0.09	14	62	8	36	*[4]	*[4]	0.352	8.94	0.040	1.0	0.311	7.90
	6	Double JR	0.18	61	270	62	280	46	205	0.424	10.8	0.099	2.5	0.325	8.26
B	7	DR Bars	0.11	39	175	34	150	26	530	0.310	7.87	0.032	0.81	0.278	7.06
	5	Single JR	0.09	46	205	45	200	36	160	0.470	11.9	0.040	1.0	0.384	9.75
C	9	DR Bars	0.11	76	340	58	260	*[3]	*[3]	1.496[5]	38.0	0.472[5]	12.0	1.024	26.01
	10	Double JR	0.18	90	400	81	360	*[4]	*[4]	0.642	16.3	0.189	4.80	0.453	11.5
D	3	DR Bars	0.11	50	220	34	150	*[4]	*[4]	0.333	8.46	0.027	0.69	0.306	7.77
	4	Single JR	0.09	84	375	68	300	*[4]	*[4]	0.492	12.5	0.051	1.3	0.442	11.2
	8	Double JR	0.18	68	300	66	295	7	31	0.334	8.48	0.030	0.76	0.304	7.72

[1]Average shear values for primary and reverse loading, interpolated between loading cycle peaks.
[2]For 8'-8" (2,642 mm) wall height, story drifts are: 0.728 in. (18.5 mm), 1.04 in. (26.4 mm), and 2.08 in. (52.8 mm), respectively.
[3]Failure of vertical reinforcement did not allow the level of drift to occur
[4]Test was not taken to the displacement required or test frame interfered with test results
[5]Data based on one direction of test only

Shear Walls 1 and 2 experienced significant sliding, but much later in the tests. Shear Wall 3 through 8 experienced only small sliding displacements. Shear Walls 9 and 10 developed a plane of failure at the base resulting in sliding prior to peak load. Displacements due to sliding may not be as effective in dissipating energy as other modes of deformation, visible in the envelopes for Shear Walls 1, 2, and 9. However, provided stability is not compromised, sliding can allow significant dissipation of energy and structure flexibility to avoid collapse.

Load-Displacement Envelopes and Ductility

There are significant advantages to comparing envelopes of load-displacement loops rather than plots of load-cycle loops. Load-displacement envelopes allow easy comparison of wall strength and behavior, allowing visualization of parameters that relate directly to the computation of ductility and collapse resistance. Envelopes for the load-displacement curves for each wall group are provided in Figures 11(a) through 11(d). The primary and reverse loading directions are the positive and negative displacement curves, respectively.

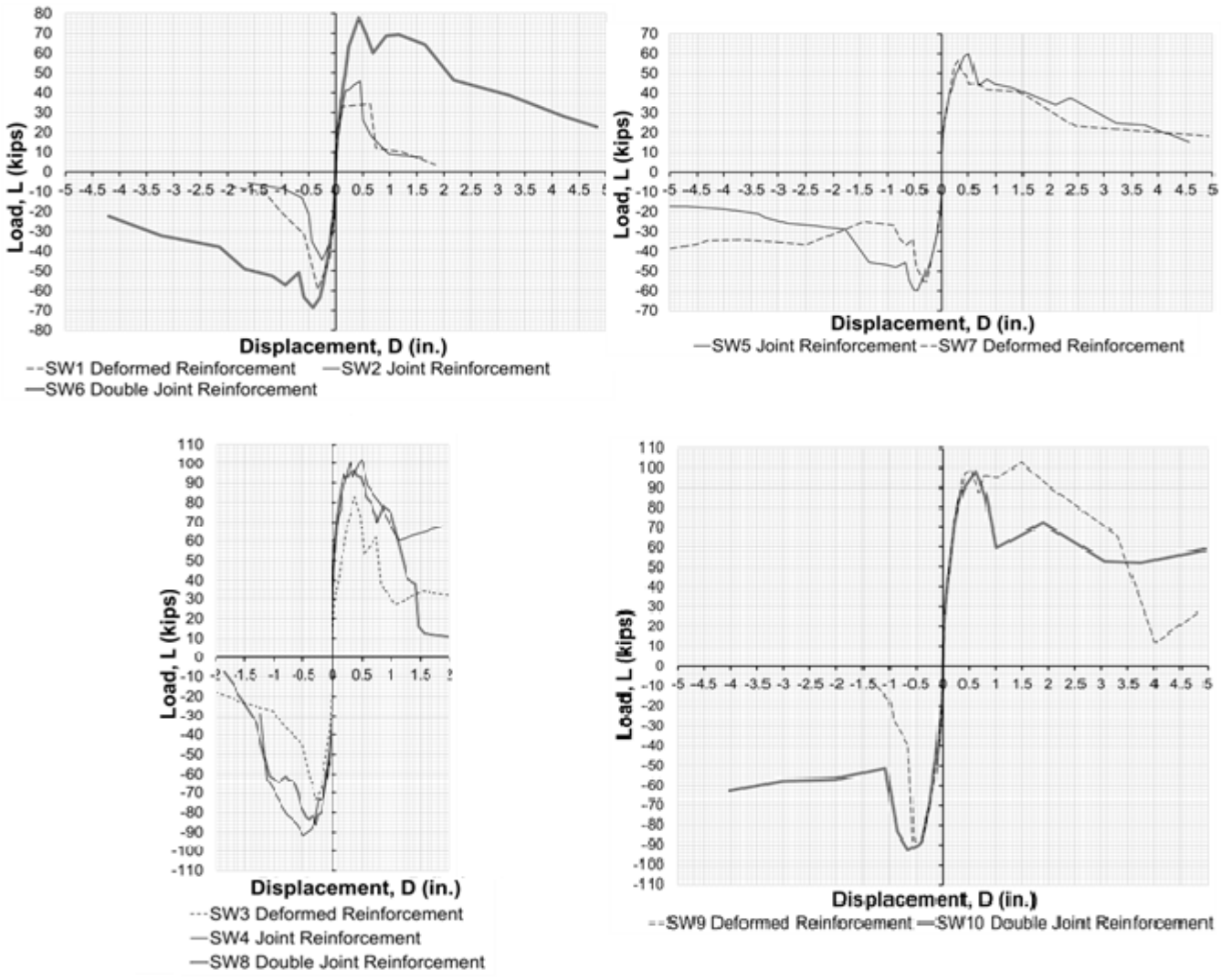

Figure 11 – Envelopes of Peak Load Cycle Data: (a) Group A (upper left); (b) Group B (upper right); (c) Group C (lower right); and (d) Group D (lower left)

The primary and reverse envelopes for Wall Group A, Figure 11(a), are similar except for load capacity and the plateau in the primary direction for Shear Wall 1. This behavior was due to the vertical jamb bar anchorage failure in the top bond beam. The envelopes for Group B Shear Walls 5 and 7, Figure 11(b), are all similar. The greater capacity, ductility, and energy dissipation of Shear Wall 5 is evident, as well as, the greater uniformity of behavior in both loading directions. The Envelopes for Shear Wall Group C, Figure 11(c), fully grouted walls are significantly stiffer and stronger than the partially grouted walls with the same aspect ratio. The envelopes for Group D, Figure 11(d), with lower aspect ratio, were also significantly stiffer and stronger than the other partially grouted walls; resulting in smaller displacement at peak load and the overall drift capacity. The greater initial stiffness and more gradual damage, due to jambs remaining elastic and due to the longer shear failure plane, resulted in higher ductilities.

The displacement ductility, μ_d, in FEMA P695 (ATC (2009)), is the ratio of ultimate displacement, δ_u, to effective yield displacement, $\delta_{y,eff}$, Figure 12(a). Ductility relates the proximity of collapse due to strength degradation to plastic yielding and is associated with the wall's ability to dissipate energy through plastic deformations. Larger values of ductility implied larger overall drift capacity prior to collapse and increased likelihood of wall survival in a seismic event.

The percentage of shear capacity used to determine collapse and effective yield is not specified in FEMA P695 (ATC, 2009). The percentage of maximum shear capacity used to represent the point of collapse in concrete structures is usually 80%. Based on NIST GCR 01-808 (Schultz (2001)), a criterion of 75% may be appropriate for softer masonry structures. Deformation capacity is based on the load resistance dropping permanently below 75% of capacity. The criterion for the effective yield intercept is 40% of maximum shear based on the inverse of the 2.5 overstrength factor for masonry from ASCE 7-10 (ASCE (2010)). Ductility is illustrated in Figure 12(b) from FEMA P695 (ATC (2009)).

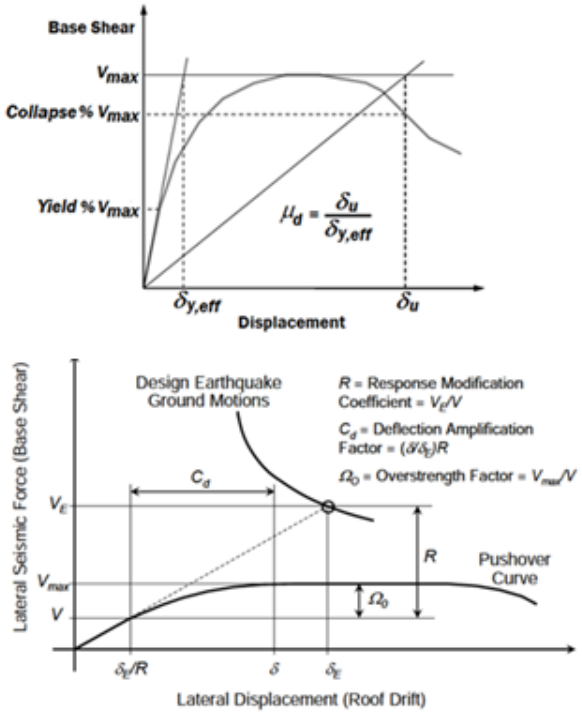

Figure 12 – (a) Illustration of Displacement Ductility (μ_d) for Load-Displacement Envelopes (top) FEMA P695 (ATC 2009) and (b) Relationship Between Design Shear, V, and Overstrength, Ω_0, (bottom)

Table 5. Ductility Comparison by Group Based on Various Yield Criteria[1] with Sliding Included and Removed[3]

		Yield Criterion	75%		67%		40%				Effective Inelastic			
		Sliding	Included						Removed		Included		Removed	
		Overstrength	1.33		1.5		2.5				Varies			
Group	Wall	Reinforcement	P[3]	R[3]	P[3]	R[3]	P[3]	R[3]	P[3]	R[3]	P[3]	R[3]	P[3]	R[3]
A	1	DR	-[4]	2.94	-[4]	4.90	-[4]	4.37	-[4]	4.0	-[4]	3.4	-[4]	3.1
	2	Single JR	3.11	3.07	3.68	3.29	4.70	5.01	4.2	4.1	2.7	3.3	2.4	2.2
	6	Double JR	6.32	4.00	6.37	4.21	8.66	7.08	8.7	7.1	6.3	3.3	6.3	3.3
B	7	DR	3.02	2.17	3.28	2.50	8.23	5.18	8.2	5.2	2.6(2.46)[5]	1.7(2.04)[5]	2.6(2.46)[5]	1.7(2.04)[5]
	5	Single JR	2.61	2.83	3.58	3.22	6.78	6.43	6.8	6.4	3.9(2.53)[5]	2.0(2.30)[5]	3.9(2.53)[5]	2.0(2.30)[5]
C	9	DR	-[4]	2.04	-[4]	2.42	-[4]	3.27	-[4]	3.0	-[4]	1.4(2.72)[5]	-[4]	1.1(2.21)[5]
	10	Double JR	2.44	2.71	2.84	2.95	6.81	6.67	4.0	3.1	3.9(5.65)[5]	3.2(4.98)[5]	1.9(2.81)[5]	1.3(2.03)[5]
D	3	DR	1.90	2.64	2.30	3.10	4.75	5.09	4.7	5.1	1.7	2.2	1.7	2.2
	4	Single JR	4.51	4.72	6.58	6.55	13.4	18.0	13.4	18.0	5.6	5.0	5.6	5.0
	8	Double JR	7.71	3.48	10.2	5.31	23.2	16.4	23.2	16.4	4.9	2.9	4.9	2.9

[1]The 40% yield criterion is based on ASCE (2010) overstrength and FEMA P695 criteria (ATC 2009) for ductility.
[2]The effective inelastic yield criteria are based on estimations of the point of transition from elastic to plastic wall behavior.
[3]Loading directions provided: P – Primary direction (+ displacement and direction loaded first), and R – Reverse direction.
[4]The ductility evaluation for SW1 and SW9 was not provided due to failures, as indicated above and in Baenziger, 2010.
[5]Ductilities based on the yielding of flexural steel, where it occurred, are provided in parentheses following the values computed using the effective inelastic yield criteria.

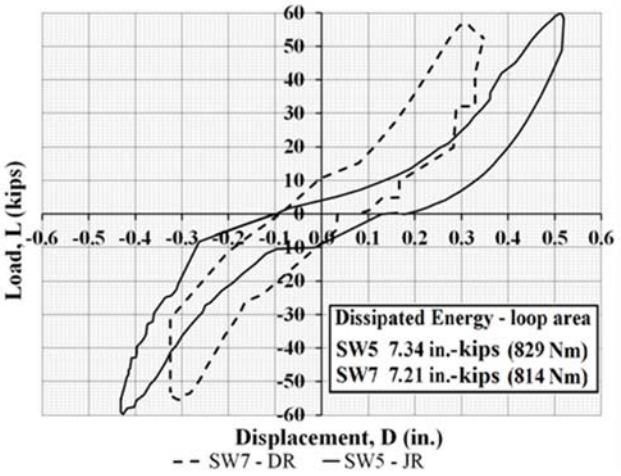

Figure 13 – Peak Load Loops for SW5 and SW7. The loop areas are almost equal indicating that energy dissipation in the walls is nearly equivalent.

The ductilities provided in Table 5 have been computed using several criteria, which differ in the manner of determining effective yield. Historically, a fixed percentage of maximum shear capacity was used to define the effective yield point, which provided a relative comparison of ductility. Four of the walls, Shear Walls 5, 7, 9 and 10, were configured to be conventional in design, with the flexural steel yielding as required and with design loads corresponding to the 40% criterion.

An "Effective Inelastic Yield Criteria" is also included, based on an estimate of the transition between elastic and inelastic behavior. The method is subjective and can be based on different criteria and thus is not recommended for comparison of wall designs. The method used here involves visual identification of a change in stiffness in the load-displacement data to determine the point of yield. The approach results in values that are typical of higher fixed percentage criteria, which are not consistent with conventional masonry shear wall design and the ASCE overstrength criteria.

Where the overstrength criterion is met in conventional designs, including Shear Walls 5, 7, 9 and 10, comparison of ductility can be made based on yielding of the vertical reinforcement. The remaining walls are shear dominated walls, in which flexural steel yielding did not occur, and are designed to remain elastic for the life of the structure. Ductilities based on the yield of flexural steel are provided in parentheses in Table 5.

Energy Dissipation Potential

Energy dissipated due to a combination of displacements, plastic deformations, cracking, crushing, and sliding of masonry shear wall components can be sufficient to avoid collapse caused by seismic loading, provided the walls are sufficiently ductile and do not have a brittle mechanism for failure. Failure mechanisms can include toe crushing, excessive sliding, jamb delaminating, fracture of reinforcement, buckling or other instability.

Analysis of the data, without normalization, indicates that the energy dissipation of walls with joint reinforcement is of a similar magnitude to comparable walls with deformed reinforcement in bond beams. The comparison was made by computing the energy capacity of peak loops and by integrating the energy capacity of the full load-displacement envelopes. The areas integrated in this manner provide a reasonable comparison of the total work acting on the walls in the loading protocol, which is designed to mimic a seismic event that exceeds the capacity of the wall. The area within a loop represents the net energy dissipated. A plot comparing the peak load loops from Shear Walls 5 and 7 is provided in Figure 13.

The summary of the dissipated energies computed from the areas under the load-displacement envelopes is provided in Table 6. The areas beneath the envelopes are representative of the cumulative energy dissipated during the entire wall test and thus indicate the wall energy resistance to collapse. The energy capacities of walls with joint reinforcement are, in general, greater than or equal to walls with deformed reinforcement.

Table 6. Envelope Energy Based on Area Under the Envelope of Load-Displacement Loops[1]

Group	Wall	Type	Total		Prime(+disp.)		Reverse(-disp.)	
			in.-kips	Joules	in.-kips	Joules	in.-kips	Joules
A	1	DR	79.3	8960	32.2	3640	47.1	5320
	2	JR	58.6	6620	30.9	3490	27.7	3130
	6	2JR	401.1	45320	227.1	25660	174.0	19660
B	7	DR	312.9	35350	155.2	17540	157.7	17820
	5	JR	315.3	35620	146.0	16500	169.2	19120
C	9	DR	384.5	43440	326.4	36880	58.1	6560
	10	2JR	558.4	63090	311.3	35170	247.2	27930
D	3	DR	154.2	17420	84.8	9580	69.4	7840
	4	JR	228.8	25850	139.4	15750	89.4	10100
	8	2JR	207.2	23410	111.3	12580	95.9	10800

[1]Presentation of original data without normalization

Summary of Behavioral Observations

The shear capacity of walls with joint reinforcement was approximately equal to or greater than that of walls with deformed reinforcement. Based on averaged wall strengths of comparable walls, walls with joint reinforcement are 9% stronger than the corresponding walls with deformed reinforcement. The walls with joint reinforcement had a greater number of smaller cracks and more uniform distribution and size of cracks than the walls with deformed reinforcement. The walls with joint reinforcement acted as a whole, whereas, the upper half of the walls with the mid-height bond beam behaved separately from the lower half. The average ductility and energy dissipation of walls with joint reinforcement was greater than or approximately equal to those walls with deformed reinforcement. The energy dissipated in the peak loop of the wall with joint reinforcement exceeded the energy dissipated in the peak loop of the wall with deformed reinforcement.

CONCLUSIONS

There are many important conclusions that can be drawn from these tests. Specifically and in detail:

1. For many common design conditions, joint reinforcement can provide the necessary capacity and ductility required as the primary shear reinforcement for shear walls.
2. Walls with joint reinforcement performed as well as or better than walls with bond beams.
3. Single ladder style 3/16-inch (4.8-mm) joint reinforcement spaced at 8 inches (203 mm) can replace two #4 (M#13) deformed reinforcement bars in bond beams spaced at 48 inches (1.22 m) in partially grouted shear walls.
4. Double seismic style joint reinforcement, four 3/16-inch (4.8-mm) wires, spaced at 8 inches (203 mm) can replace two #4 (M#13) deformed reinforcement bars spaced at 48 inches (1.22 m) in partially grouted and fully grouted shear walls.
5. Unlike some historical tests discussed in the Background Section, the areas of joint reinforcement used in this research provided the strength required to resist the shear loads up to failure by other mechanisms.
6. Well distributed 3/16-inch (4.8-mm) double seismic style joint reinforcement provided the strength and ductility required to resist seismic level cyclic loading.
7. The 3/16-inch (4.8-mm) ladder style joint reinforcement at 8-inch (203-mm) spacing provided superior crack control over bond beams containing 2 #4 (M#13) bars at 48-inch (1.22-m) spacing.
8. The 8-inch (203-mm) joint reinforcement spacing limited the size of cracks and resulted in a larger number of smaller cracks across the wall (as opposed to a smaller number of larger cracks).
9. Mobilization of reinforcement is improved in walls with closely spaced joint reinforcement.
10. Sufficient areas of horizontal shear reinforcement are required to provide the necessary shear strength to avoid the fracture that occurred in earlier historical shear wall tests cited in the Background Section of this paper.
11. Additional areas of reinforcement provided beyond that required for strength do not add to the strength of the wall, but do reduce or delay wall damage if well distributed, and thereby can increase wall ductility.
12. Masonry prism strength varied; however, greater prism strength combined with less reinforcement resulted in less ductility.

RECOMMENDATIONS

The results suggest that joint reinforcement should be included in masonry codes for use as primary shear reinforcement with appropriate limits placed upon the material properties to ensure that the necessary strain capacity, compatibility, and strength are obtained. Certain construction details are recommended to increase inelastic deformation capacity and to delay undesirable failure modes until well past the collapse level deformations for both walls with deformed reinforcement and walls with joint reinforcement. The detailed recommendations for shear walls are as follows.

1. Horizontal joint reinforcement and deformed reinforcement should be anchored using hooks around the vertical reinforcement in the grouted jambs to develop the shear reinforcement. Joint reinforcement should have cross wires and bent longitudinal wires anchored in the grouted cells.
2. Vertical reinforcement should be anchored at or above the top of the wall to avoid tension pullout of the vertical reinforcement.
3. Reinforcement and grout should be placed in the first two jamb end cells.
4. In shear walls with low surcharge, vertical reinforcement above the plastic hinge region in jamb cells should be increased to maintain elastic behavior, thereby allowing cracks to close each cycle.
5. Intermediate vertical reinforcement should be provided in grouted pairs of cells, thereby providing column-like rigid cell frame behavior in the reinforced portions of partially grouted shear walls.
6. The spacing of vertical reinforcement should be reduced if only single reinforcement and grouted cells are used, Nolph (2011).
7. In experimental evaluation of performance, Air-cured prisms should be used and cured adjacent to their shear walls rather than wet-cured prisms to provide a more accurate measure of the strength of masonry for comparison with code predicted capacities.

ACKNOWLEDGMENTS

The work associated with this paper was conducted by Iowa State University under the auspices of the Engineering Research Institute, with sponsorship provided by Hohmann & Barnard, Inc., Wire-Bond, Inc., and Dayton Superior, Inc. The authors wish to thank the sponsors for their consultation, time, and resources donated. The authors also wish to thank the Masonry Institute of Iowa (MII), Forrest and Associates, The Industry Advisory Panel chaired by Mario Catani, The Consultants Advisory Panel, Laboratory Supervisor Doug Wood, and student assistants from the Department of Civil, Construction and Environmental Engineering.

REFERENCES

ASCE (2010). American Society of Civil Engineers, "Minimum Design Loads for Buildings and Other Structures," ASCE Standard 7-10, ASCE/SEI, Reston, VA, 2010.

ASTM (2006). American Society for Testing and Materials (ASTM), "Annual Book of ASTM Standards," including: C90-06 Specification for Loadbearing Concrete Masonry Units; C109/C109M-07 Test Method for Compressive Strength of Hydraulic Cement Mortars; A153/A153M-09 Specification for Zinc Coating (Hot-Dip) on Iron and Steel Hardware; C270-00 Specification for Mortar for Unit Masonry; C476-02 Specification for Grout for Masonry; A615/A615M-09b Specification for Deformed and Plain Carbon-Steel Bars for Concrete Reinforcement; A951/A951M-06 Specification for Steel Wire for Masonry Joint Reinforcement; C1019-03 Test Method for Sampling and Testing Grout; and C1314-03b Test Method for Compressive Strength of Masonry Prisms; ASTM International, www.astm.org, West Conshohocken, PA, 2006.

ATC (2009). Applied Technology Council, "Quantification of Building Seismic Performance Factors – FEMA P695," June 2009.

Baenziger et al. (2010a). Baenziger, G. P., Porter, M. L., "In-Plane Structural Testing of Joint Reinforcement in Concrete Masonry Shear Walls," Iowa State University, Ames, IA, April 2010.

Baenziger et al. (2010b) Baenziger, G. P., Porter, M. L., "In-Plane Structural Testing of Joint Reinforcement in Concrete Masonry Shear Walls – Supplement 1: Potential Code Provisions," Iowa State University, Ames, IA, 2010.

Baenziger et al. (2011). Baenziger, G. P., Porter, M. L., "Joint Reinforcement for Masonry Shear Walls," 11th North American Masonry Conference, Minneapolis, MN, The Masonry Society, Longmont, CO, June 2011.

Baenziger et al. (2012). Baenziger, G. P., Porter, M. L., "In-Plane Structural Testing of Joint Reinforcement in Concrete Masonry Shear Walls – Supplement 2: Comparison of Experimental Results to Design Capacity," Iowa State University, Ames, IA, March 2012.

Braun (1997). "Bond and Strain Behavior of Horizontal Reinforcement in Masonry Mortar Joints", Masters Thesis, Iowa State University, Ames, IA,1997.

MSJC (2008)."Building Code Requirements for Masonry Structures, Specification for Masonry Structures, and Commentaries," Masonry Standards Joint Committee, The Masonry Society, Longmont, CO; 2008.

Harris (2010). Harris, B. H., "Investigation of the Lower Bound Compressive and Flexural Strengths of Conventional Concrete and Clay Masonry," Master's Thesis, University of Texas, Arlington, TX, 2010.

Nolph et al. (2011). Nolph, S. M., ElGawady, M. A., "In-Plane Shear Strength of Partially Grouted Masonry Shear Walls," 11th North American Masonry Conference Proceedings, Minneapolis, MN, The Masonry Society, Longmont, CO, June 2011.

Porter (1987). Porter, M. L. "Sequential Phased Displacement (SPD) Procedure for TCCMAR Testing," Proceedings of Third Meeting of the Joint Technical Coordinating Committee on Masonry Research of the U.S., Japan Coordinated Earthquake Research Program, Sapporo, Japan, October 1987.

Porter et al. (1998). Porter, M. L., Braun, R. A., "Horizontal Reinforcement Elongation in Masonry Mortar Joints," Proceedings, Eighth Canadian Masonry Symposium, pp. 599-609, Jasper, Canada, Canadian Masonry Research Institute, Mississauga, ON, May 1998.

Porter et al. (1999). Porter, M. L., Braun, R. L., "An Effective Gage Length for Joint Reinforcement in Masonry," Proceedings of Eighth North American Masonry Conference, Austin, Texas, The Masonry Society, Longmont, CO, June, 1999.

Schultz (1994). Schultz, A. E., "NIST Research Program on the Seismic Resistance of Partially Grouted Masonry Shear Walls," NISTIR 5481, Building and Fire Research Laboratory, National Institute of Standards and Technology, Gaithersburg, MD, June 1994.

Schultz (1996). Schultz, A. E., "Minimum Horizontal Reinforcement Requirements for Seismic Design of Masonry Walls," TMS Journal, Vol. 14, pp. 53-64, The Masonry Society, Longmont, CO, 1996.

Schultz et al. (1998). Schultz, A. E., Hutchinson, R. S., Cheok, G. C., "Seismic Performance of Masonry Walls with Bed Joint reinforcement," T119-4, Elsevier Science Ltd., Amsterdam, Netherlands,1998.

Schultz et al. (2001). Schultz, A. E., Hutchinson, R. S., "Seismic Behavior of Partially-Grouted Masonry Shear Walls: Phase 2 – Effectiveness of Bed-Joint reinforcement," NIST GCR 01-808, Building and Fire Research Laboratory, Dept. of Civil Engineering, University of Minnesota, Minneapolis, MN, 2001.

Shing et al. (1989). Shing, P.B., Noland, J. L., Klamerus, E., Spaeh, H., "Inelastic Behavior of Concrete Masonry Shear Walls," Vol. 115, No. 9, ASCE Journal of Structural Engineering, Reston, VA, September 1989.

Shing et al. (1990). Shing, P.B., Schuller, M., Hoskere, V.S., "In-Plane Resistance of Reinforced Masonry Shear Walls," Vol. 116, No. 3, ASCE Journal of Structural Engineering, American Society of Civil Engineers (ASCE), Reston, VA, March 1990.

Shing et al. (1991). Shing, P.B., Noland, J.L., Spaeh, H.P., Klamerus, E.W., and Schuller, M.P., "Response of Single-Story Reinforced Masonry Shear Walls to In-Plane Lateral Loads," Report No. 3.1(a)-2, U.S.- Japan Coordinated Program for Masonry Building Research, Dept. of Civil, Environmental, and Architectural Engineering, University of Colorado, Boulder, CO, 1991.

Shing et al. (1992). Shing, P. B., Noland, J. L., "Shear Behavior of Concrete Masonry Walls with Horizontal Joint Reinforcement" Report for sponsors: Dur-O-Wal and the National Science Foundation, University of Colorado, Boulder, CO, 1992.

Sveinsson et al. (1985). Sveinsson, B. I., McNiven, H. D., Sucuoglu, H., "Cyclic Loading Tests of Masonry Single Piers - Volume 4; Additional Tests with Height to Width Ratio of 1," UCB/EERC-85/15, Earthquake Engineering Research Center, University of California, Berkeley, CA, December 1985.

NOTATION

2JR = Double joint reinforcement (seismic style)

A_{gross} = Gross Area of masonry

$A_{s\ Horz}$ = Area of Horizontal reinforcement steel

$A_{s\ Vert}$ = Area of Vertical reinforcement steel

d or d_v = Depth of wall effective in resisting shear

δ_u = Ultimate displacement at collapse

$\delta_{y,eff}$ = Displacement at effective yield

DR = Deformed Reinforcement

f'_m = Specified Masonry Design Strength

$f'_{m\text{-}prism}$ = Experimental Wet Prism Strength

JR = Joint reinforcement

(M#16) = Soft Metric bar size 16 mm (U.S. #5 bar)

$M/(Vd)$ = Shear wall aspect ratio used in MSJC

M = Moment at the base of a shear wall

μ_d = Displacement ductility

Ω_0 = Overstrength

P = Primary load direction (+ displacement)

R = Reverse load direction (- displacement)

ρ_h or ρ_{horz} = Horizontal reinforcement ratio ($A_{s\ horz}/A_{gross}$)

ρ_{vert} = Vertical reinforcement ratio ($A_{s\ vert}/A_{gross}$)

TCCMAR = Joint Technical Coordinating Committee on Masonry Research

V = Shear load applied at the top of a shear wall

V_{max} = Maximum shear load capacity